Physics of high-pressure helium and argon radio-frequency plasmas

M. Moravej, X. Yang, G. R. Nowling, J. P. Chang, and R. F. Hicks[a)]
Chemical Engineering Department, University of California, Los Angeles, California 90095

S. E. Babayan
Surfx Technologies LLC, 3617 Hayden Avenue, Culver City, California 90232

(Received 19 January 2004; accepted 22 September 2004)

The physics of helium and argon rf discharges have been investigated in the pressure range from 50 to 760 Torr. The plasma source consists of metal electrodes that are perforated to allow the gas to flow through them. Current and voltage plots were obtained at different purity levels and it was found that trace impurities do not affect the shape of the curves. The electron temperature was calculated using an energy balance on the unbound electrons. It increased with decreasing pressure from 1.1 to 2.4 eV for helium and from 1.1 to 2.0 for argon. The plasma density calculated at a constant current density of 138 mA/cm^2 ranged from 1.7×10^{11} to 9.3×10^{11} cm^{-3} for helium and from 2.5×10^{11} to 2.4×10^{12} cm^{-3} for argon, increasing with the pressure. At atmospheric pressure, the electron density of the argon plasma is 2.5 times that of the helium plasma. © *2004 American Institute of Physics*. [DOI: 10.1063/1.1815047]

I. INTRODUCTION

Plasmas are used in materials manufacturing for a diverse range of processes, including surface activation, etching, cleaning, decontamination, and thin film coatings.[1,2] Industrial plasmas operate either at low pressure (<2 Torr) or at atmospheric pressure. Examples of low-pressure plasmas are capacitive discharges, inductively coupled plasmas, and electron cyclotron resonance sources.[2,3] Atmospheric pressure discharges fall into two main categories: thermal plasma torches, which exhibit gas temperatures exceeding 3000 °C,[4,5] and nonequilibrium discharges, which run at near room temperature.[6,7] Torches are limited in application to substrates that are not thermally sensitive. In addition, they require high voltage transformers and high currents to maintain the discharge.[8,9] The most common low-temperature, atmospheric pressure plasmas are dielectric barrier discharges (DBD) and coronas. These devices are powered by dc or high frequency supplies operating up to 20 kHz.[6,7] A thin dielectric barrier is placed on one of the electrodes to prevent the formation of a continuous arc. These plasmas normally exhibit short-lived micro arcs that are randomly distributed in space and time.[10] However, they can be made to produce a uniform glow by operating the DBD in pure helium, argon, or nitrogen.[11–17]

We have developed an atmospheric pressure plasma that is stabilized by helium or argon and operates at temperatures below 100 °C.[18–28] This source utilizes perforated metal electrodes that are coupled to radio frequency power at 13.56 MHz. The plasma discharge generates a uniform, high density of atoms and radicals for materials processing. So far we have demonstrated the use of this device for the plasma-enhanced chemical vapor deposition of silicon dioxide, silicon nitride, and amorphous hydrogenated silicon.[19–21] In addition, it has been applied to the etching of kapton, tantalum, silicon, and uranium oxide.[22–25] One of the unique properties of the plasma is that it operates at pressures from 10 to 760 Torr without any modifications to the electrode design.

Recently, a study has been conducted on the physics of an rf, atmospheric pressure discharge stabilized by helium.[26] In this source, the gas flowed parallel to two closely spaced metal electrodes. The electron density and temperature were determined to be 3×10^{11} cm^{-3} and 1.9 eV at a current density of 30 mA/cm^2.[27] The current-voltage characteristics of the plasma were measured, and it was found that the voltage was independent of the current in the normal glow regime. A theoretical study of this plasma by Yuan and Raja[29] suggested that impurities on the level of 5 ppm were necessary to explain the shape of the current-voltage curves.

In this paper, we investigate the physics of helium and argon plasmas utilizing perforated metal electrodes that are coupled to an rf power supply. A pressure range from 30 to 760 Torr has been examined in this study. The feed gases have been carefully purified so that the effect of impurities on the current-voltage characteristics may be assessed. Furthermore, calculations have been made to determine the plasma density and electron temperature as a function of the inert gas type and total pressure.

II. EXPERIMENTAL METHODS

A schematic of the experimental apparatus is shown in Fig. 1. An Atomflo™-250 plasma source from Surfx Technologies LLC was used in these experiments. The discharge was produced between two perforated, circular aluminum electrodes, 2.5 cm in diameter, containing 150 holes. A picture of the plasma operating with pure helium is shown in the figure as well. The spacing between the electrodes was 1.6 mm, but was modified in some of the experiments to either 0.4 or 2.4 mm. Gas was fed upstream of the discharge and allowed to flow through the electrodes and out into a variable pressure chamber. The plasma was maintained by supplying rf power at 13.56 MHz to the top electrode, while

a)Electronic mail: rhicks@ucla.edu

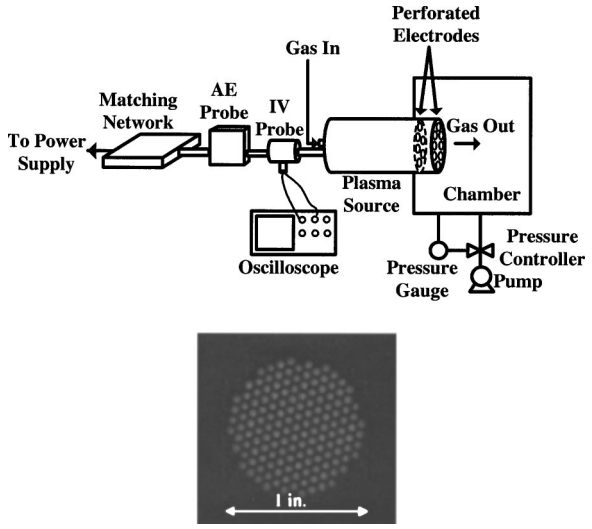

FIG. 1. Schematic of the experimental apparatus (not to scale) and picture of the plasma source.

the bottom electrode was grounded. A current and voltage (*IV*) probe was attached directly to the source, eliminating any cable connections, which might add inductance to the system. This probe was connected to an oscilloscope (Tektronix, TDS 224). An additional tuned impedance probe (Advanced Energy RFZ 60) was inserted in the line between the matching network and the *IV* probe. The plasma voltage as a function of current was determined with the Advanced Energy probe, which also yielded information on the impedance, resistance, and phase angle. The *IV* probe was used to determine the time-dependent current and voltage wave forms.

The plasma source was mounted on an ultrahigh vacuum chamber that was connected to a mechanical pump and a pressure controller. The chamber was fitted with a window facing the discharge, through which optical emission spectra were obtained. The pressure range examined was from 50 to 760 Torr. A SAES getter was used to purify the helium and argon gases to <10 parts per billion (ppb) prior to introduction into the plasma source. Optical emission spectra of the plasma were obtained to check that the gas contained negligible impurities. A comparison of the emission spectra between ultrahigh purity helium (<1000 ppm) and this gas passed through the SAES getter is shown in Fig. 2. For the former case, oxygen was detected as the main impurity, as observed by the O II peaks at 391.2 and 427.5 nm and the OH peak at 309.0 nm.[30,31] When the purifier was turned on these lines disappeared, indicating that the oxygen had been removed. No emission lines for species other than the He could be detected in this latter spectrum.

The neutral gas temperature of the helium plasma at 760 Torr was determined by adding 0.1 Torr nitrogen into the discharge. The light was collected through a monochromator (Instruments S.A., Triax 320), equipped with a 1200 groove/mm grating and a liquid nitrogen cooled charge-coupled device (CCD) detector (Instruments S.A., CCD-3000). The monochromator entrance slit was set to 0.05 mm resulting in a spectral resolution of 0.27 nm. The rotational temperature of the (3,0) band of the N_2 first positive emission spectrum was fitted to a Boltzmann plot, from which the gas temperature was calculated.[32] The details of this experiment have been published elsewhere.[28]

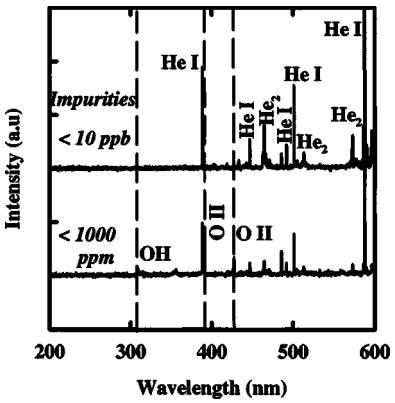

FIG. 2. Optical emission spectra of UHP helium at 300 Torr with and without additional purification.

III. RESULTS

A. Paschen curves

The Paschen curves for the helium and argon rf plasmas are shown in Fig. 3. These curves were obtained by varying the pressure from 1 to 760 Torr and using three different gap spacings, 0.4, 1.6, and 2.4 mm. The general shape of these curves agrees with that obtained for dc discharges.[2,33] The helium plasma exhibits a minimum breakdown voltage at a PD of about 4 Torr cm. In dc discharge using an aluminum electrode, the minimum breakdown voltages for helium and argon are at 1.3 and 0.3 Torr cm, respectively.[2] Our helium results agree with the dc counterpart. However, the minimum value for argon could not be ascertained. Evidently, lower pd values need to be investigated that are outside the range available with our apparatus. Nevertheless, it should be pointed out that the Paschen curves were obtained in the same device with minimal adjustments, a capability that is unique for this plasma source.

B. Current and voltage Relationships

The root mean square (rms) values of the current and voltage wave forms for a helium discharge operated at 300 Torr and 2.0 W/cm^2 are shown in Fig. 4. The wave

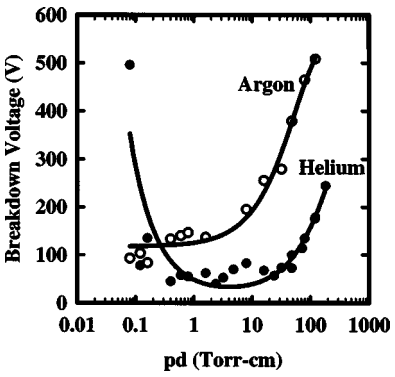

FIG. 3. Paschen curves for helium and argon rf discharges.

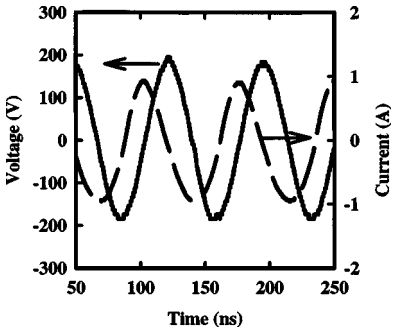

FIG. 4. Current and voltage wave forms for He at 300 Torr and 10 W.

form indicates a capacitive discharge because the phase angle between the current and the voltage is ≈86°. The 4° shift in phase angle is due to the resistive component arising from the ionized gas.[34] Analogous wave forms were obtained for the discharge in the pressure range of 100–760 Torr. They are not shown here because the only difference between these is the magnitude of the current and voltage, which increase with pressure.

Current and voltage wave forms obtained for argon at 2.0 W/cm^2 and 300 Torr are shown in Fig. 5. The argon plasma is also capacitive with the current leading the voltage by 79°. The phase angle is shifted further for Ar than for He, indicating that the Ar plasma exhibits a higher resistance. Another difference between the helium and argon plasmas is that in the latter case the current wave form is not smooth but has a kink in it. A possible reason for this could be due to the harmonics associated with this plasma.[35]

Current-voltage curves for helium at pressures from 100 to 760 Torr are shown in Fig. 6. The points on the curves indicate the breakdown voltages. The lines correspond to abnormal glow operation. By convention, abnormal glow corresponds to the region where the voltage rises with the current, while normal glow defines the region where the voltage is constant.[2] Beyond the end of the lines the plasma transforms into a filamentary arc. The plasma is turned off at this point, because in an arc the current is concentrated on a small area of the electrode and prolonged exposure can damage it. At all pressures, the discharge operates over a current range spanning ≈0.55 A. The operating voltage decreases substantially as the pressure is reduced, because at lower pressures less power is needed to sustain the discharge.

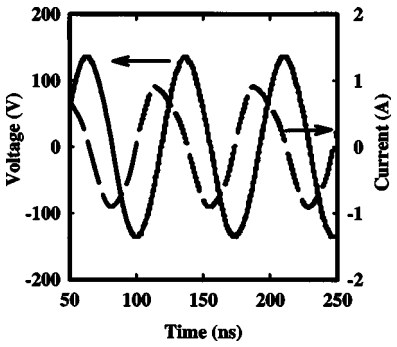

FIG. 5. Current and voltage wave forms for Ar at 300 Torr and 10 W.

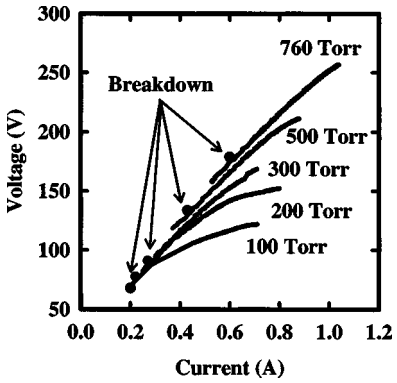

FIG. 6. Voltages as a function of current for a He discharge at different pressures.

Current-voltage plots for the abnormal glow regime of the argon discharge are shown in Fig. 7. The breakdown voltages are not shown on this plot, but they vary over a wide range from 510 V at 760 Torr to 240 V at 100 Torr. From these curves, one can see that the argon plasma operates at a lower potential than the helium plasma, even though its breakdown voltage is substantially higher. The biggest difference between the helium and argon discharges is the *IV* curve at 760 Torr. The helium plasma exhibits a smooth curve with a wide operating range of 0.5 A, whereas the argon plasma shows a narrow operating range of only 0.1 A. Moreover, the Ar plasma at atmospheric pressure exhibits streamers and is not stable. We do not know the reason for this behavior and further work is underway to characterize this phenomenon.

To examine the effect of trace amounts of impurities on the shape of the *IV* curves, data has been obtained for four different impurity levels, 1.3 vol%, 0.05 vol%, 1000 ppm, and <0.01 ppm. The highest impurity level corresponds to adding 10 Torr of O_2 to the helium gas. The plots shown in Figs. 6 and 7 are for He and Ar with <0.01 ppm of impurities. Experiments performed for 0.05 vol% and 1000 ppm do not exhibit any differences to the ones for <0.01 ppm, so these are not shown here. The current-voltage plots for the plasma fed with 750 Torr helium and 10 Torr oxygen are shown in Fig. 8. The difference between these results and those of Fig. 6 is that the addition of O_2 increases the break-

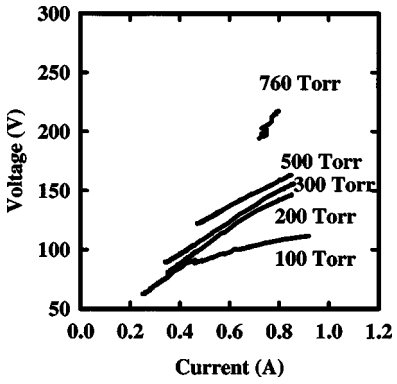

FIG. 7. Voltages as a function of current for an Ar discharge at various pressures.

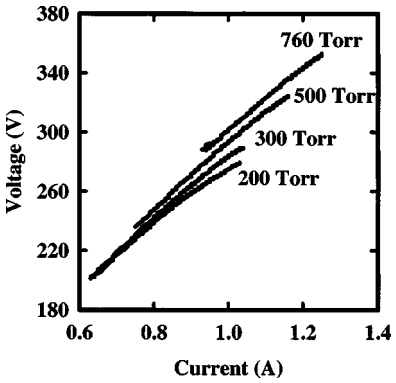

FIG. 8. Voltages as a function of current for a He/O_2 plasma at various pressures.

down voltage and the operating voltage. However, the shape of the *IV* curve does not change, the voltage gradually increases with the current.

C. Plasma parameters

The plasma density and electron temperature have been determined for both the helium and argon plasmas. The plasma density is calculated from the following equation:

$$J = -en_e\mu_e E, \tag{1}$$

where J is the current density (A/m^2), e is a unit charge (C), μ_e is the electron mobility (V/m s, which is dependent on the gas medium and is inversely proportional to the pressure), E is the bulk electric field (V/m), and n_e (m^{-3}) is the electron density. The average electron temperature is calculated from a steady-state power balance on the free electrons in the plasma:[31,36]

$$\epsilon = n_e\frac{P}{K_B T_g}k_1 I_1 + n_e n_{a^*} k l_{a^*} n_e\left[n_e\langle\sigma_{ei}\nu_e\rangle + \frac{P}{K_B T_g}\langle\sigma_{ea}\nu_e\rangle + n_{a^*}\langle\sigma_{ea^*}\nu_e\rangle\right]\frac{2m_e}{M}\frac{3}{2}K_B(T_e - T_g) - \epsilon_{\text{rad}}, \tag{2}$$

where ϵ is the power density (W/m^3), ϵ_{rad} is the energy loss due to radiation (W/m^3), P is the pressure (Pa), T_g is the gas temperature (eV), T_e is the electron temperature (eV), k_1 is the ionization rate coefficient (which is a function of T_e), and I_1 is the first ionization energy (eV). In this equation a^* represents the first excited state of the atom, k is the rate coefficient of ionization from the excited state (m^2/s), I_{a^*} is the ionization energy of a^*, and $\langle\sigma_{ei}\nu_e\rangle$, $\langle\sigma_{ea}\nu_e\rangle$, and $\langle\sigma_{ea^*}\nu_e\rangle$ are the electron-ion, electron-atom, and electron-excited state collision rate coefficients (which are functions of n_e and T_e), respectively.

The first two terms on the right-hand side of Eq. (2) are due to inelastic collisions between electrons and other species. It should be noted that a range of values were found for k, the ionization rate coefficient from the excited state, so all of them were utilized in the calculations and only minute differences were observed in the n_e and T_e calculations.[37–41] Although the inelastic electron collisions with the excited states of He and Ar are taken into account, their rate was found to have a minimal effect on the T_e calculation. This is because in the pressure range examined, the density of the excited and metastable species is negligible compared to the ground state (<1000 ppb). This conclusion was drawn by calculating the density of the excited species, i.e., Ar(4s) and He($2p$), using the method described by Jonkers *et al.*[42–44]

To account for the energy losses due to radiation, the losses due to ion free-free interactions (Bremsstrahlung), recombination, and line transitions were calculated using the expressions developed by Benoy *et al.* for nonequilibrium plasmas.[42,45,46] It was found that the addition of this loss term to Eq. (2) did not change the calculated T_e value. To demonstrate this point, the total radiative losses were calculated at a T_e of 2 eV and n_e of 10^{11} cm^{-3}, yielding a value of $\approx 4\times10^{-6}$ W/m^3, which is negligible compared to the total input power density of 2.3×10^7 W/m^3. The electron energy balance indicates that the power input per unit volume is lost due to elastic and inelastic electron collisions.

To examine how much of the power input goes into heating the gas, a simple thermal energy balance has been performed:

$$\varepsilon = \frac{\dot{m}c_p\Delta T}{\overline{V}}. \tag{3}$$

Here, $\overline{V}$ it the volume of the plasma gas (m^3), m is the mass flow rate (kg/s), c_p is the specific heat capacity (J/mol K) and ΔT is the change in gas temperature (K). The mass flow rate was determined from the volumetric flow rate, which was 30 L/min at 24°C and 760 Torr. The outlet temperature of the gas was determined using emission spectroscopy. At a power input of 20 W, the neutral gas temperature in the plasma is found to be 63°C. From these values, it is calculated that the power consumed to heat the gas from 24 to 63°C is 17 W, accounting for 85% of the input power. The remaining 3 W is probably lost by radiation and by transport to the surroundings from the body of the plasma souree. If it is assumed that the entire 3 W is lost due to radiation and this value is input into Eq. (2), the new T_e calculated for He and Ar at atmospheric pressure is 1.10 eV, as compared to 1.14 and 1.12 eV, respectively. This difference is less than 4%, therefore it can be seen through this method also that the radiation losses are negligible compared to the total power input.

The sheath thickness is calculated using the equations developed for a collisional sheath:[2,47]

$$J = 1.68\epsilon_0\left(\frac{2e\lambda_i}{M}\right)^{1/2}\frac{V^{3/2}}{s^{5/2}}. \tag{4}$$

Here, ϵ_0 is the permittivity of vacuum (F/m), V is the voltage (V), M is the molecular weight of the rare gas ion, He^+ or Ar^+ (kg/mol), λ_i is the mean free path of the ion (m), and s is the total sheath thickness (m). From the sheath thickness, the sheath capacitance may be calculated as follows:

$$C = \frac{1.52\epsilon_0 A}{s}, \tag{5}$$

where A is the electrode are (m^2). Finally, the voltage drop across the sheath is given by

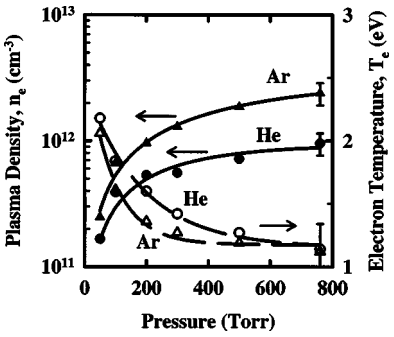

FIG. 9. Electron density and temperature for the helium and argon plasmas as a function of pressure at a constant current density of 138 mA/cm^2.

$$V = \frac{I}{2\pi f C}, \tag{6}$$

where I is the total current supplied (A) and f is the frequency (Hz). Knowing the sheath thickness and voltage drop allows one to calculate the plasma parameters for the bulk region only. The calculated thickness obtained for helium and argon between 50 and 760 Torr were 0.14–0.08 mm and 0.07–0.04 mm, respectively.

To check the calculations used to determine the sheath thickness and voltage drop across it, the electric field for the bulk plasma was calculated at two gap spacings, 1.6 and 2.4 mm. The electric field at a fixed current density is only a function of pressure and plasma density and is independent of the gap spacing. From the *IV* data, the sheath properties were calculated from Eqs. (4)–(6), and then used to estimate the electric field of the bulk plasma. These fields for the 1.6 and 2.4 mm gaps were always within 20% of each other over the range of pressures studied, from 100 to 760 Torr. Since the bulk electric fields are relatively unaffected by the gap spacings, one may assume that the sheath calculations are valid.

From the formulas given above, the plasma density and electron temperature were calculated at a fixed current of 0.7 Å (138 mA/cm^2). The results of these calculations for the helium and argon discharges are shown in Fig. 9. The plasma density increases from $1.6\pm0.3\times10^{11}$ to $9.3\pm1.8\times10^{11}$ cm^{-3} for helium, and from $2.5\pm0.5\times10^{11}$ to $2.4\pm0.5\times10^{12}$ cm^{-3} for argon as the pressure rises from 50 to 760 Torr. Meanwhile, the T_e decreases from 2.4 ± 0.4 to 1.1 ± 0.2 eVand from 2.1 ± 0.4 to 1.1 ± 0.2 eV as the pressure increases from 50 to 760 Torr, for helium and argon, respectively. Note that over this pressure range the helium sheath thickness varies from 0.14 to 0.08 mm. For the argon plasma, the sheath thickness does not vary with pressure, maintaining an average value of ~0.05 mm. The electron temperature falls at higher pressures, because the electrons collide more frequently with neutrals and ions and loose their energy faster.[48] In contrast, the plasma density rises with pressure. According to Eq. (1), the density is inversely proportional to the electron mobility and the electric field. The mobility decreases and the field increases as the pressure rises. However, the mobility variation is ten times larger than that of the electric field, so it has a stronger influence on the density.

We have calculated the properties of the helium plasma containing 1.3 vol% oxygen. In Eq. (2), the physical parameters for helium were used since it is the dominant species. It was found that at a fixed current density of 200 mA/cm^2, n_e increases from 1.6×10^{11} to 5.6×10^{11} cm^{-3}, while T_e decreases from 1.9 to 1.3 eV as the pressure rises from 200 to 760 Torr. Thus, while higher input powers are required to sustain the oxygen and helium discharge, it appears that the addition of O_2 reduces the electron density by a factor of 2, but has minimal effect on the electron temperature. The reduction on the plasma density is most likely due to the fact that O_2 is an electronegative species so it consumes the electrons and therefore lowers their concentration.[49,50]

IV. DISCUSSION

We have investigated the properties of high-pressure helium and argon discharges that are sustained by flowing the gas through perforated metal electrodes. The *IV* curves for helium and He/O_2 presented in Figs. 6 and 8 indicate that this design provides a broad range of currents for operation. In particular, the current density at 760 Torr varies from a minimum of 70 mA/cm^2 following breakdown to a maximum of 190 mA/cm^2 at the arcing point. We have performed the same measurements on the parallel plate system that was previously studied by Park *et al.*[26] In that case, the current density varies from 10 mA/cm^2 at breakdown to 30 mA/cm^2 at the arcing point. This is a much narrower operating range than found in the present case.

In Park's work with the parallel plate electrodes, it was found that the voltage did not change with the current over the normal glow operating regime.[26] The model calculations of Yuan and Raja[29] suggested that this behavior could be attributed to the presence of impurities in the discharge at a level of ~5 ppm. However, we have studied the effect of impurities on the helium plasma and have shown that for up to 1.3 vol% O_2 there is no effect on the shape of the *IV* curves (cf. Fig. 8).

An alternative explanation for the flat *IV* curve observed in Park's study is that it may have been characteristic of their particular electrode design. In the present work, the electrodes are circular with an area of 5.1 cm^2 and the gas flows through them. When the gas undergoes breakdown, the plasma immediately fills the entire volume between the electrodes. Upon applying more power to this system, the current density increases and hence the plasma potential rises.[2,33] By contrast, the source used by Park contained rectangular electrodes with an area of 100 cm^2 and the gas flowed in between them.[26] We have found that when this design is employed, the plasma does not fill the entire gas volume after breakdown. Instead, as more power is applied to the electrodes, the discharge expands, so that the current per unit area, and in turn the plasma potential, remains relatively constant.

The current voltage characteristics of the pure helium discharge recorded herein are consistent with the results of a theoretical modeling study performed by Yuan and Raja.[29] They showed that the voltage increases monotonically with the current, exhibiting a slope of 60 V/A. This may be com-

pared to a value of 190 V/A measured for the perforated electrodes. On the other hand, our results do not agree with theirs in the case where the gas contains impurities. We have found that with up to 1.3 vol% O_2 in He, there is no effect on the *IV* curve.

The electron density and temperature of the helium and argon discharges were calculated using equations for electron current and a power balance on free electrons, respectively. It was found that the helium plasma density increased from $1.7\pm0.3\times10^{11}$ to $9.3\pm1.8\times10^{11}$ cm^{-3} as the pressure rose from 50 to 760 Torr, whereas the argon density increased from $2.5\pm0.5\times10^{11}$ to $2.5\pm0.5\times10^{12}$ cm^{-3} in the same range. The electron density in the argon plasma was 1.5–2.5 larger than that of the helium discharge. This can be explained by comparing the first ionization energies of the neutral atoms, 24.6 eV for helium and 15.8 eV for argon. Argon is easier to ionize so at the same average electron temperature, it will have a higher electron concentration.[2]

Note that the plasma density is inversely proportional to the electron mobility, which is equal to the electron drift velocity multiplied by the electric field. Both discharges operate at similar electric fields, however the electron drift velocity in argon is two to three times smaller than that in helium (0.8×10^6 cm/s versus 0.4×10^6 cm/s at 760 Torr).[51–53] According to Eq. (1), the lower mobility of electrons in the argon medium is compensated for by a higher plasma density.[51–53] These results agree with low pressure, weakly ionized discharges, where argon plasmas exhibit electron densities of 10^{10} cm^{-3} compared to $\sim10^9$ cm^{-3} for helium plasmas.[54–59]

The atmospheric pressure helium and argon discharges were used to etch positive-tone photoresist (AZ-5214E). The etch process was a remote one, where the substrate was not in direct contact with the plasma but only with the afterglow. The conditions used were 10 W total power (2 W/cm^2), 0.05 vol% O_2, 25 L/min total flow rate, 1000 rpm, and 3 mm electrode-to-substrate spacing. At these conditions, the ash rates were 70 and 185 Å/min for helium and argon, respectively. We have shown that when an oxygen plasma is used for etching, the active species are ground state oxygen atoms.[22,23] Therefore, the faster etch rate with argon may be explained by looking at the electron-impact dissociation of the oxygen molecule:[2]

$$e + O_2 \rightarrow 2O + e \quad k = 4.2\times10^{-9}e^{-5.6/Te}. \tag{R1}$$

The rate of O atom production is $r=kn_en_{O_2}$, where n_{O_2} is the oxygen concentration. Based on the n_e and T_e values observed at atmospheric pressure, the O atom production rates are 2.9×10^{18} cm^3/s for the He plasma and 6.8×10^{18} cm^3/s for the Ar plasma. The latter rate is 2.5 times faster, which is in agreement with the 2.6 times higher etching rate in argon.

Since the plasma source contains perforated electrodes, there is some question as to whether it may operate like a hallow cathode discharge with the plasma sustained within the holes. We do not have a definite answer for this point, although our data suggest that the plasma is uniformly distributed over the gas volume between the gap in the electrodes. In addition, most hollow cathode discharges reported in literature are configured with the cathode and anode separated by a dielectric material that fills the gap.[60–63] By contrast, the plasma design investigated herein does not employ dielectric material. Several groups have performed model calculations and experiments and determined that there is a range of pressure times hole diameters, where the hollow cathode effect is valid.[60–63] The maximum pd reported is 10 Torr cm. In the present work, the pd values range from 8.0 to 60.0 Torr cm, and are for the most part, outside the range expected for a hollow cathode discharge.

V. CONCLUSIONS

We have investigated the physics of a capacitively coupled radio-frequency plasma source operating at pressures from 50 to 760 Torr. In pure helium, the electron density increases with pressure from 1.7×10^{11} to 9.3×10^{11} cm^{-3}, while the electron temperature decreases with pressure from 2.4 to 1.1 eV. Over the same pressure range, the argon plasma exhibits essentially the same electron temperatures, but a factor of 2.5× higher electron densities. This may be attributed to the lower ionization energy and electron mobility of argon compared to helium. Impurity levels of 1.3 vol% or less have no effect on the plasma properties, contrary to previously published results.

ACKNOWLEDGMENTS

This work was supported by grants from the U. S. Department of Energy, Environmental Management Sciences Program (Grant No. FG07-00ER45857), the University of California Discovery Grant No. (ele 10123), Surfx Technologies, LLC, and AMD. The authors would like to thank Joel Penelon for his valuable input.

[1] J. R. Roth, *Industrial Plasma Engineering: Principles* (Institute of Physics, Berkshire, 1995).
[2] M. A. Lieberman and A. J. Lichtenberg, *Principles of Plasma Discharges and Materials Processing* (Wiley, New York, 1994).
[3] F. F. Chen, *Introduction to Plasma Physics and Controlled Fusion* (Plenum, New York, 1984).
[4] P. Fauchais and A. Vardelle, IEEE Trans. Plasma Sci. **25**, 1258 (1997).
[5] R. W. Smith, D. Wei, and D. Apelian, Plasma Chem. Plasma Process. **9**, 135S (1989).
[6] M. Goldman and R. S. Sigmond, IEEE Trans. Electr. Insul. **17**, 90 (1982).
[7] J. S. Chang, P. A. Lawless, and T. Yamamoto, IEEE Trans. Plasma Sci. **19**, 1152 (1991).
[8] S. Ramakrishnan and M. W. Rogozinski, J. Phys. D **30**, 636 (1997).
[9] S. Ramakrishnan, M. Gershenzon, F. Polivka, T. N. Kearney, and M. W. Rogozinski, IEEE Trans. Plasma Sci. **25**, 937 (1997).
[10] B. Eliasson and U. Kogelschatz, IEEE Trans. Plasma Sci. **19**, 1063 (1991).
[11] F. Massines and G. Gouda, J. Phys. D **31**, 3411 (1998).
[12] F. Massines, A. Rabehi, P. Decomps, R. B. Gadri, P. Segur, and C. Mayoux, J. Appl. Phys. **83**, 2950 (1998).
[13] N. Gherardi and F. Massines, IEEE Trans. Plasma Sci. **29**, 536 (2001).
[14] T. C. Montie, K. Kelly-Wintenberg, and J. R. Roth, IEEE Trans. Plasma Sci. **28**, 41 (2000).
[15] I. Radu, R. Bartnikas, G. Czeremuszkin, and M. R. Wertheimer, IEEE Trans. Plasma Sci. **31**, 411 (2003).
[16] U. Kogelschatz, IEEE Trans. Plasma Sci. **30**, 1400 (2002).
[17] F. Massines, G. Gouda, N. Gherardi, M. Duran, and E. Croquesel, Plasmas Polymers 6, 35 (2001).
[18] A. Schütze, J. Y. Jeong, S. E. Babayan, J. Park, G. S. Selwyn, and R. F. Hicks, IEEE Trans. Plasma Sci. **26**, 1685 (1998).
[19] S. E. Babayan, J. Y. Jeong, A. Schütze, V. J. Tu, M. Moravej, G. S. Selwyn, and R. F. Hicks, Plasma Sources Sci. Technol. **10**, 573 (2001).

[20]G. R. Nowling, S. E. Babayan, V. Jankovic, and R. F. Hicks, Plasma Sources Sci. Technol. **11**, 97 (2002).
[21]M. Moravej, S. E. Babayan, G. R. Nowling, X. Yang, and R. F. Hicks, Plasma Sources Sci. Technol. **13**, 8 (2004).
[22]J. Y. Jeong, S. E. Babayan, V. J. Tu, I. Henins, J. Velarde, G. S. Selwyn, and R. F. Hicks, Plasma Sources Sci. Technol. **7**, 282 (1998).
[23]J. Y. Jeong, S. E. Babayan, A. Schütze, V. J. Tu, J. Y. Park, I. Henins, G. S. Selwyn, and R. F. Hicks, J. Vac. Sci. Technol. A **17**, 2581 (1999).
[24]V. J. Tu, J. Y. Jeong, A. Schütze, S. E. Babayan, G. Ding, G. S. Selwyn, and R. F. Hicks, J. Vac. Sci. Technol. A **18**, 2799 (2000).
[25]X. Yang, M. Moravej, S. E. Babayan, G. R. Nowling, and R. F. Hicks, J. Nucl. Mater. **324**, 134 (2004).
[26]J. Park, I. Henins, H. W. Herrmann, G. S. Selwyn, and R. F. Hicks, J. Appl. Phys. **89**, 20 (2001).
[27]J. Park, I. Henins, H. W. Herrmann, and G. S. Selwyn, Phys. Plasmas **7**, 3134 (2000).
[28]S. E. Babayan, G. Ding, and R. F. Hicks, Plasma Chem. Plasma Process. **21**, 505 (2001).
[29]X. Yuan and L. L. Raja, Appl. Phys. Lett. **81**, 814 (2002).
[30]J. Reader, C. H. Corliss, W. L. Wiese, and G. A. Martin, *Wavelengths and Transition Probabilities for Atoms and Atomic Ions* (U. S. Government Printing Office, Washington, DC, 1980).
[31]R. W. B. Pearse and A. G. Gaydon, *The Identification of Molecular Spectra* (Wiley, New York, 1950).
[32]M. Simek and S. De Benedictis, Plasma Chem. Plasma Process. **15**, 451 (1995).
[33]Y. P. Raizer, M. N. Shneider, and N. A. Yatsenko, *Radio-Frequency Capacitive Discharge* (CRC, Boca Raton, FL, 1995).
[34]J. W. Nilsson and S. A. Riedel, *Electric Circuits* (Prentice-Hall, Englewood Cliffs, NJ, 2000).
[35]V. A. Godyak, R. B. Piejak, and B. M. Alexandrovich, IEEE Trans. Plasma Sci. **19**, 660 (1991).
[36]M. Mitchner and C. H. Kruger, Jr., *Partially Ionized Gases* (Wiley, New York, 1973).
[37]J. W. Shon and M. J. Kushner, J. Appl. Phys. **75**, 1883 (1994).
[38]F. Kannari, A. Suda, M. Obara, and T. Fujioka, IEEE J. Quantum Electron. **QE-19**, 1587 (1983).
[39]J. M. Ajello, G. K. James, B. Franklin, and S. Howell, J. Phys. B **23**, 4355 (1990).
[40]K. Tachibana, Phys. Rev. A **34**, 1007 (1986).
[41]R. Deloche, P. Monchicourt, M. Cheret, and F. Lambert, Phys. Rev. A **13**, 1140 (1976).
[42]J. Jonkers, M. van de Sande, A. Sola, A. Gamero, and J. Van der Mullen, Plasma Sources Sci. Technol. **13**, 30 (2003).
[43]J. Jonkers and J. A. M. Van der Mullen, J. Quant. Spectrosc. Radiat. Transf. **61**, 703 (1999).
[44]J. A. M. Van der Mullen, Phys. Rep. **191**, 109 (1990).
[45]D. A. Benoy, J. A. M. Van der Mullen, and D. C. Schram, J. Phys. D **26**, 1408 (1993).
[46]G. M. Jansesen, J. van Dijk, D. A. Benoy, K. T. A. L. Burm, W. J. Goedheer, J. A. M. Van der Mullen, and D. C. Schram, Plasma Sources Sci. Technol. **8**, 1 (1999).
[47]M. A. Lieberman, IEEE Trans. Plasma Sci. **17**, 338 (1989).
[48]E. W. McDaniel, *Collision Phenomena in Ionized Gases* (Wiley, New York, 1964).
[49]E. Kändler, G. Graβhoff, and K. Drescher, Surf. Coat. Technol. **74-75**, 539 (1995).
[50]A. M. Diamy, N. Gonzalez Flesca, and J. C. Legrand, Spectrochim. Acta, Part B **41**, 317 (1986).
[51]Y. P. Raizer, *Gas Discharge Physics* (Springer, Berlin, 1987).
[52]B. M. Smirnov, *Physics of Weakly Ionized Gases* (Mir, Moscow, 1981).
[53]S. C. Brown, *Basic Data of Plasma Physics* (The M.I.T Press, Cambridge, MA, 1967).
[54]P. Belenguer, J. P. Blondeau, L. Boufendi, M. Toogood, A. Plain, A. Bouchoule, C. Laure, and J. P. Bouef, Phys. Rev. A **46**, 7923 (1992).
[55]C. Penache, M. Miclea, A. Bräuning-Demian, O. Hohn, S. Schössler, T. Jahnke, K. Niemax, and H. Schmidt-Böcking, Plasma Sources Sci. Technol. **11**, 476 (2002).
[56]K. Dzierżęga, K. Musioł, E. C. Benck, and J. R. Roberts, J. Appl. Phys. **80**, 3196 (1996).
[57]L. D. Biborosch, O. Bilwatsch, S. Ish-Shalom, E. Dewald, U. Ernst, and K. Frank, Appl. Phys. Lett. **75**, 3926 (1999).
[58]S. Yan, H. Kamal, J. Amundson, and N. Hershkowitz, Rev. Sci. Instrum. **67**, 4130 (1996).
[59]E. I. Toader, W. G. Graham, C. M. O. Mahony, and P. G. Steen, Rev. Sci. Instrum. **73**, 2974 (2002).
[60]K. H. Schoenbach, R. Verhappen, T. Tessnow, F. E. Peterkin, and W. W. Byszewski, Appl. Phys. Lett. **68**, 13 (1996).
[61]K. H. Schoenbach, A. El-Habachi, W. Shi, and M. Ciocca, Plasma Sources Sci. Technol. **6**, 468 (1997).
[62]M. T. Ngo, K. H. Schoenbach, G. A. Gerdin, and J. H. Lee, IEEE Trans. Plasma Sci. **18**, 669 (1990).
[63]A. Melzer, R. Flohr, and A. Piel, Plasma Sources Sci. Technol. **4**, 424 (1995).